BLOOD VESSEL EXTRACTION FROM OCT DATA BY SHORT-TIME RPCA

Pin-Hsien Lee[⋆]*, Chin-Cheng Chan*[⋆]*, Sheng-Lung Huang*[⋆]*, Andrew Chen*[†]*, and Homer H. Chen*[⋆]

[⋆] National Taiwan University
[†]David Geffen School of Medicine at UCLA

ABSTRACT

Optical coherence tomography (OCT) is a medical imaging technology that allows for non-invasive diagnosis of diseases in the early stage. Because blood flow anomalies provide useful information for many diseases, we develop an automatic blood vessel detection algorithm based on the robust principle component analysis (RPCA) technique. Specifically, we propose a short-time RPCA method that divides an OCT volume into segments and decomposes each segment into a low-rank structure representing relatively static tissues and a sparse matrix representing the blood vessels. It efficiently extracts blood vessel structure from OCT data by distinguishing static and dynamic components. This work serves as the foundation for further blood flow analysis.

Index Terms— OCT, RPCA, biomedical image processing

1. INTRODUCTION

Optical coherence tomography (OCT) is a promising medical imaging technology that has been widely used in various medical fields. OCT has gained much attention from researchers and doctors since the early nineties when the technology was first adopted by ophthalmologists for non-invasive *in vivo* medical analysis with micron resolution [1]. OCT plays a role in assessing vision impairment caused by diseases like glaucoma or age-related macular degeneration [2], [3]. OCT is also adopted in various medical fields such as cardiology and dermatology [4], [5].

OCT images reveal the underlying structure of live biological tissue by measuring the light reflected from the specimen. The longitudinal position of the reflection sites are determined by low-coherence interferometry. A depth profile, so called A-scan, of the sample point is generated. Conventional OCT systems acquire a depth scan from one sample point at one point in time. To generate a volume data of the specimen, the sample arm of an OCT system has to move transversally, thus introducing time delay between acquisitions. Although modern commercial OCT systems can perform hundreds of thousands A-scans per second, the slight delay can still result in significant motion artifact, which results in image discontinuity introduced by unexpected movements of the specimen. On the other hand, full-field optical coherence tomography (FF-OCT) acquires images in a transverse plane or *en face* images [6]. The design ensures all pixels in any transverse plane of FF-OCT volume data are generated at the same time point. Thus each *en face* image is free of motion artifact.

In this paper, we propose a short-time RPCA algorithm to extract blood vessels from FF-OCT data and show that the proposed algorithm outperforms traditional RPCA. The performance of this vascular structure visualization algorithm is subjectively compared with other methods, including RPCA.

The remainder of this paper is organized as follows. Section 2 discusses previous work and Section 4 describes our algorithm for automatic blood vessel detection. Experiment results are presented in Section 5, and finally we conclude our work in Section 6.

2. VISUALIZATION OF CAPILLARIES

Visualizing vascular structure is important in medical applications. Many approaches to visualization and measurement of blood flows have been proposed for conventional OCT systems [7]–[10]. The blood flow velocity is measured by the Doppler frequency shift of the back-scattered light [7] or the phase variance of the OCT data [8], [9]. Enfield et al. [10] introduced the correlation mapping optical coherence tomography (cmOCT) technique to extract the blood vessels from OCT images and reported that the dynamic components in OCT images tend to have a lower correlation coefficient than the relatively static components.

Here, we investigate the problem of extracting blood vessels using FF-OCT data. McNamara et al. [11] applied the cmOCT technique [10], which is originally developed for conventional OCT, to the FF-OCT data of a tadpole in the tail region. We tackle the blood vessel extraction problem by RPCA, a technique that has gained much attention in the field of image processing but has not been used to extract blood vessels from OCT data before.

3. OCT DATA DESCRIPTION

Figure 1 shows an example of the OCT volume data generated from the FF-OCT system with an axial and lateral resolution

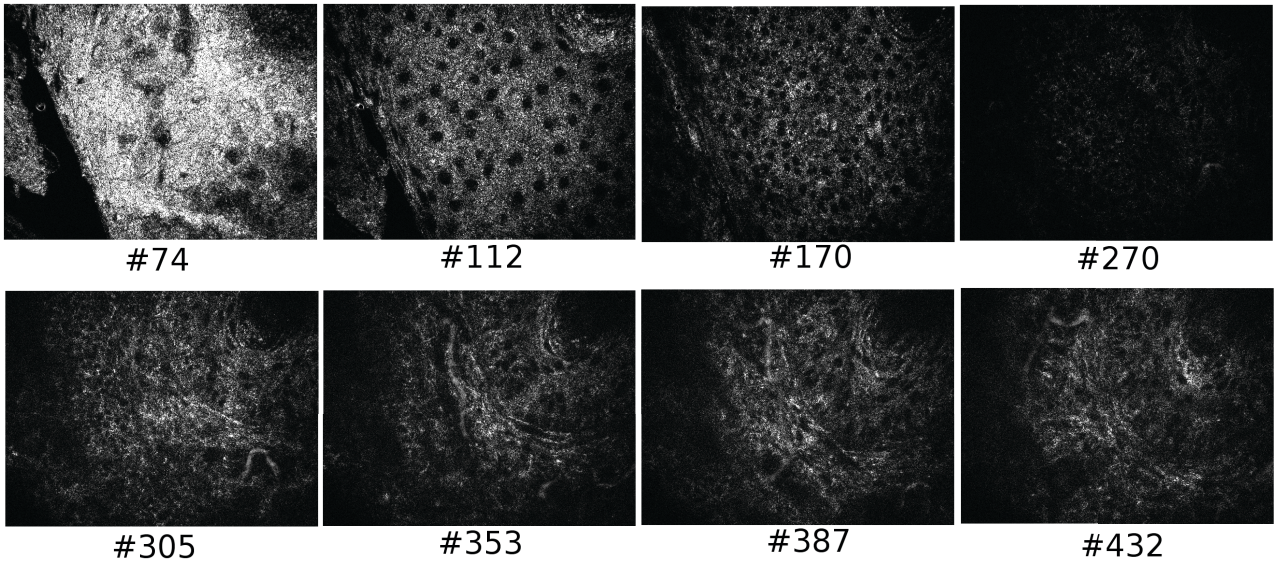

Fig. 1: Eight sample images of a volume of OCT data for testing. Top row: the *en face* slices of epidermis. Bottom row: the *en face* slices of dermis. The intensity of the bottom images is scaled up before display. Each image represents a 220×290 micron square in dimension (488×648 pixels). The depth separation between images is 0.2 micron.

of 0.9 μm and 0.8 μm, respectively [12]. This OCT volume records a three-dimensional tissue structure of human face skin from a 25-year-old Asian male subject, with a frame separation of 0.2 μm. The top row shows the anatomic structure of epidermis, and the bottom row shows the anatomic structure of dermis, where the capillary network exists. Note that the light reflected from deeper tissues is weaker than those from more superficial tissues. The intensity of dermis region is lower than the epidermis region. For better visualization, the intensity of the sample images of dermis is scaled up.

The frame number below each image indicates the chronological order captured by the FF-OCT system. Since the FF-OCT system begins its *en face* image acquisition from the surface of skin, the larger the frame number, the deeper the tissue it reveals.

4. BLOOD VESSEL DETECTION VIA SHORT-TIME RPCA

In an OCT image sequence, red blood cells constitute the moving part while the other tissues are the static part. Even though static tissue moves gradually as the depth of each frame varies, red blood cells move much faster than the other tissues. Thus, the blood vessels can be distinguished from the background by speed of movement. The OCT images share a huge amount of common information and only differ from each other by sparse errors. In other words, the image sequence can be decomposed into a low-rank structure and a matrix of sparse errors.

4.1. Problem formulation

Consider an OCT image sequence composed of k images. Each image has size $m \times n$. If we vectorize each image and stack the k images together, we obtain a matrix D with size $mn \times k$, where D is a low rank matrix. The blood vessel detection can be formulated as an optimization problem,

$$\underset{A}{\operatorname{argmin}} \ rank(A) + \lambda ||E||_0 \quad s.t. \quad D = A + E, \quad (1)$$

where A denotes a low-rank matrix and E denotes a sparse matrix. In this formulation, the static tissues are mathematically represented by the low-rank structure, and red blood cells are represented by the sparse matrix. However, this problem is NP-hard [13]. Fortunately, John Wright et al. [14] showed that (1) can be approximated by the following equation:

$$\underset{A}{\operatorname{argmin}} \ ||A||_* + \lambda ||E||_1 \quad s.t. \quad D = A + E, \quad (2)$$

where $||\cdot||_*$ denotes the nuclear norm of a matrix. Several algorithms have been proposed for solving the RPCA problem, and among them the inexact augmented Lagrange multiplier (ALM) [15] is one of the fastest algorithms. Thus, we adopt it in this work.

However, the above formulation can not be directly used because of the changing subspace of the matrix D (the depth of each OCT image is different). Several attempts have been made [16], [17], [18], but most of them involve a complex

RPCA formulation and is computationally expensive. In the proposed method, we use a simple but effective approach to solve the problem.

Our idea of coping with the gradually changing subspace is to use a short-time version of RPCA. It entails partitioning the original sequence into small segments of equal length, and applying RPCA to each segment. Each segment consists of a number of consecutive frames and is the input D to RPCA. This approach is reasonable because the subspace changes slowly throughout the whole sequence. In other words, the subspace preserves a low-rank structure locally. The short-time RPCA is applied to a small number of consecutive frames, thus it does not suffer much from the changing subspace. This simple approach is effective in detecting blood vessels as described in Section 5. A flowchart of the short-time RPCA is illustrated in Figure 2.

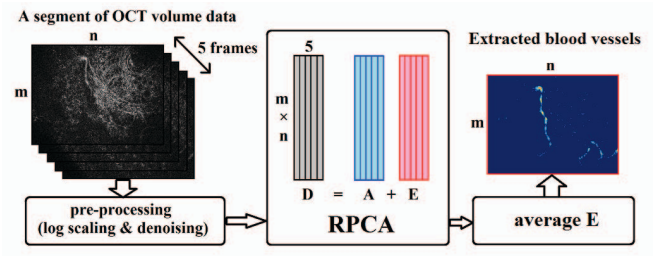

Fig. 2: A flowchart of the proposed short-time RPCA algorithm.

4.2. Image pre-processing

Most images captured by OCT have poor image quality due to noise, and the red blood cells have low-contrast. Therefore, a pre-processing procedure is needed. Specifically, we apply a logarithmic scaling to the raw image to increase the sensitivity of our algorithm to blood vessels, and a median filter to remove noise. Because both blood vessels and image noise are treated as sparse errors in RPCA, the noise removal allows us to separate blood vessels from image noise.

4.3. Output

Every five consecutive frames in an OCT dataset are grouped together to form a segment, to which the short-time RPCA method is applied. The matrix of sparse errors of a segment consists of five columns, each representing the detected blood vessels in a frame. The average of the five columns are taken as the output. The false blood vessels normally have the low intensity than the true ones. Therefore, they can be eliminated by applying an empirically determined threshold. Finally, we project the output images of each segment along the longitudinal axis to generate the blood vessel image.

5. EXPERIMENTS

We test the proposed short-time RPCA method on two OCT datasets containing images like those shown in Figure 1 and compare it with two other methods. The resolution of each dataset is $488 \times 648 \times 100$. The RPCA solver provided in [15] is used in this experiment. Our MATLAB code is run on a workstation with Intel Xeon 2.6GHz CPU without GPU acceleration.

5.1. Performance Comparison

Three methods are compared in the experiment: the cmOCT method [10], the RPCA method [15], and the short-time RPCA method. Figure 3 shows the raw OCT images and the blood vessels detected by these three methods. All images are cropped around the blood vessel for better visualization. Figures 3(a) and 3(e) are the sample *en face* images, each belonging to an OCT dataset, Figures 3(b) and 3(f) show the results generated by the cmOCT method, Figures 3(c) and 3(g) show the results generated by the RPCA method, and Figures 3(d) and 3(h) show the results generated by the short-time RPCA method.

It can be seen that Figure 3(e) is noiser than Figure 3(a) and more difficult to handle. But our method can handle them well. The blood vessels in Figures 3(d) and 3(h) are clearly extracted, but those in Figures 3(b) and 3(f) are severely degraded by background noise. Although both the RPCA method and the short-time RPCA method can produce more robust results than the cmOCT method, Figures 3(d) and 3(h) have fewer detection errors than Figures 3(c) and 3(g). This means that short-time RPCA method has better resistance to the motion of tissues surrounding the blood vessel.

We calculate the precision and recall of detected vessel region against the blood vessel mask determined manually for three different methods. The results are listed in Table 1. For the two datasets in Figure 3, the short-time RPCA has the highest precision among the three methods and obtains acceptable recall values. In terms of computational efficiency, the short-time RPCA method takes 58 seconds on the average to process a dataset of 100 OCT images, whereas the cmOCT method takes 101 seconds.

5.2. 3D view of blood vessel

A 3D view of the detected blood vessels is shown in Figures 4(a) and 5(a) for the two datasets used in the experiment. Figures 4(b) and 5(b) show the projections of the 3D blood vessels onto XY-, XZ-, and YZ-plane. Since every five consecutive OCT images form a segment in the short-time RPCA method, the depth of each 3D view is one-fifth of the original depth.

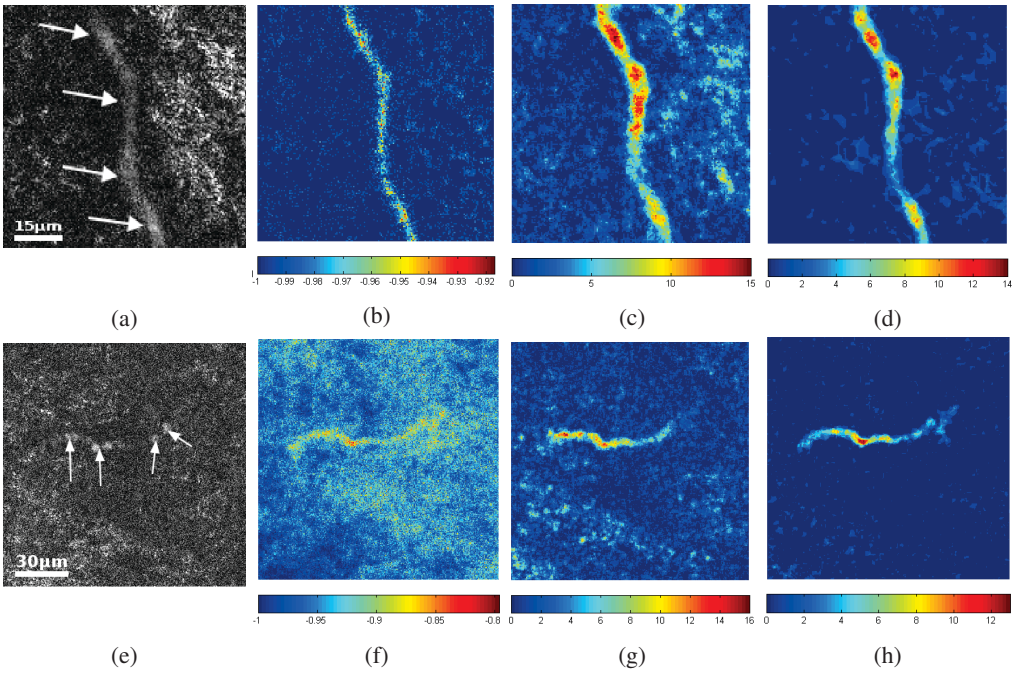

Fig. 3: Blood vessel detection. (a) The original OCT image. Bright clusters pointed to by arrows are red blood cells. The region occupied by red blood cells represents the blood vessel. (b) Result of the cmOCT method [10]. (c) Result of the RPCA method without dividing the sequence into segments. (d) Result of the short-time RPCA method by dividing the sequence into 20 segments without overlap.

Table 1: The evaluation result of the two datasets in Figure 3.

Method	Dataset #1		Dataset #2	
	Precision	Recall	Precision	Recall
cmOCT	0.3442	0.6983	0.0077	1.0000
RPCA	0.1025	0.9897	0.0346	0.9043
short-time RPCA	0.4860	0.9261	0.4277	0.7817

6. CONCLUSION

In this paper, we have described a short-time RPCA method to detect the blood vessels in FF-OCT images. The changing subspace problem is alleviated by breaking the entire dataset into small segments and processing the dataset segment by segment. Both the regular RPCA method and the short-time RPCA method are more resistant to the background noise than the cmOCT method. Also, the short-time RPCA method performs better than the regular RPCA method. The proposed method serves as the basic technique for further analysis of FF-OCT images such as blood flow estimation.

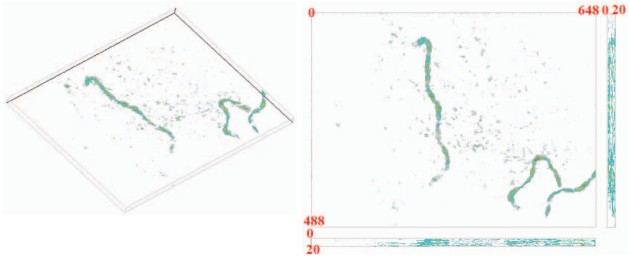

Fig. 4: (a) 3D view of the detected blood vessels for the first dataset. (b) Projections of the result onto the XY-, YZ-, and XZ- planes.

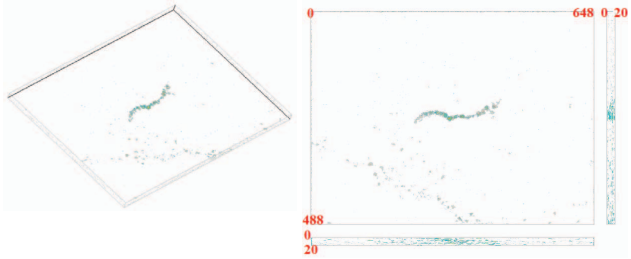

Fig. 5: (a) 3D view of the detected blood vessels for the second dataset. (b) Projections of the result onto the XY-, YZ-, and XZ- planes.

7. REFERENCES

[1] D. Huang et al., "Optical coherence tomography," *Science*, vol. 254, no. 5035, pp. 1178–1181, 1991.

[2] C. K. Leung et al., "Evaluation of retinal nerve fiber layer progression in glaucoma: a comparison between spectral-domain and time-domain optical coherence tomography," *Ophthalmology*, vol. 117, no. 12, pp. 2337–2344, 2010.

[3] P. A. Keane, P. J. Patel, S. Liakopoulos, F. M. Heussen, S. R. Sadda, and A. Tufail, "Evaluation of age-related macular degeneration with optical coherence tomography," *Survey of Ophthalmology*, vol. 57, no. 5, pp. 389–413, 2012.

[4] M. U. Farooq, A. Khasnis, A. Majid, and M. Y. Kassab, "The role of optical coherence tomography in vascular medicine," *Vascular Medicine*, vol. 14, no. 1, pp. 63–71, 2009.

[5] E. Sattler, R. Kästle, and J. Welzel, "Optical coherence tomography in dermatology," *Journal of Biomedical Optics*, vol. 18, no. 6, pp. 061224, 2013.

[6] E. Dalimier and D. Salomon, "Full-field optical coherence tomography: a new technology for 3D high-resolution skin imaging," *Dermatology*, vol. 224, no. 1, pp. 84–92, 2012.

[7] A. Bouwens, D. Szlag, M. Szkulmowski, T. Bolmont, M. Wojtkowski, and T. Lasser, "Quantitative lateral and axial flow imaging with optical coherence microscopy and tomography," *Optics Express*, vol. 21, no. 15, pp. 17711–17729, 2013.

[8] D. M. Schwartz, J. Fingler, D. Y. Kim, R. J. Zawadzki, L. S. Morse, S. S. Park, S. E. Fraser, and J. S. Werner, "Phase-variance optical coherence tomography: A technique for noninvasive angiography," *Ophthalmology*, vol. 121, no. 1, pp. 180–187, 2014.

[9] J. Fingler, R. J. Zawadzki, J. S. Werner, D. Schwartz, and S. E. Fraser, "Volumetric microvascular imaging of human retina using optical coherence tomography with a novel motion contrast technique," *Optics Express*, vol. 17, no. 24, pp. 22190–22200, 2009.

[10] J. Enfield, E. Jonathan, and M. Leahy, "In vivo imaging of the microcirculation of the volar forearm using correlation mapping optical coherence tomography (cmOCT)," *Biomedical Optics Express*, vol. 2, no. 5, pp. 1184–1193, 2011.

[11] P. M. McNamara, M. Hrebesh, and M. J. Leahy, "In vivo full-field en face correlation mapping optical coherence tomography," *Journal of biomedical optics*, vol. 18, no. 12, pp. 126008, 2013.

[12] C. C. Tsai, C. K. Chang, K. Y. Hsu, T. S. Ho, M. Y. Lin, J. W. Tjiu, and S. L. Huang, "Full-depth epidermis tomography using a Mirau-based full-field optical coherence tomography," *Biomedical Optics Express*, vol. 5, no. 9, pp. 3001–3010, 2014.

[13] E. Amaldi and V. Kann, "On the approximability of minimizing nonzero variables or unsatisfied relations in linear systems," *Theoretical Computer Science*, vol. 209, no. 1, pp. 237–260, 1998.

[14] J. Wright, A. Ganesh, S. Rao, Y. Peng, and Y. Ma, "Robust principal component analysis: Exact recovery of corrupted low-rank matrices via convex optimization," in *Advances in neural information processing systems*, 2009, pp. 2080–2088.

[15] Z. Lin, M. Chen, and Yi Ma, "The augmented lagrange multiplier method for exact recovery of corrupted low-rank matrices," *arXiv preprint arXiv:1009.5055*, 2010.

[16] C. Guyon, T. Bouwmans, and E. Zahzah, "Foreground detection based on low-rank and block-sparse matrix decomposition," in *IEEE International Conference on Image Processing*. IEEE, 2012, pp. 1225–1228.

[17] X. Zhou, C. Yang, and W. Yu, "Moving object detection by detecting contiguous outliers in the low-rank representation," *IEEE Transactions on Pattern Analysis and Machine Intelligence*, vol. 35, no. 3, pp. 597–610, 2013.

[18] S. Javed, S. Andrews, T. Bouwmans, and S. K. Jung, "OR-PCA with dynamic feature selection for robust background subtraction," in *The 30th ACM/SIGAPP Symposium on Applied Computing*, 2015.